FLAW BEHAVIOR IN MECHANICALLY LOADED CLAD PLATES*

S. K Iskander, G. C. Robinson,† and C. B. Oland†

Metals and Ceramics Division
Oak Ridge National Laboratory
Oak Ridge, Tennessee 37831-6151

ABSTRACT

A small crack near the inner surface of clad nuclear reactor pressure vessels is an important consideration in the safety assessment of the structural integrity of the vessel. Four-point bend tests on large plate specimens, six clad and two unclad, were performed to determine the effect of stainless steel cladding upon the propagation of small surface cracks subjected to stress states similar to those produced by pressurized thermal shock conditions. Test results have shown that the tough surface layer composed of cladding and/or heat-affected zone has enhanced the load-bearing capacity of plates under conditions where unclad plates have ruptured. The results are interpreted in terms of fracture mechanics. The behavior of flaws in clad reactor pressure vessels is examined in the light of the test results.

INTRODUCTION

There are considerable experimental results which have shown that, *in the absence of cladding*, a small surface flaw in an embrittled material subjected to severe thermal shock will become a long flaw.[1] However, questions remain about the role tough surface cladding will play in preventing the propagation of small flaws along the surface. Furthermore, the flaw could tunnel beneath the cladding, in which case the residual strength of the structure needs to be estimated. The question is of more than academic interest, since a small crack

*Research sponsored by the Office of Nuclear Regulatory Research, U.S. Nuclear Regulatory Commission, under Interagency Agreement DOE 1886-8011-9B with the U.S. Department of Energy under contract DE-AC05-84OR21400 with Martin Marietta Energy Systems, Inc.

†Engineering Technology Division.

near the inner surface of clad nuclear reactor pressure vessels (RPVs) is an important consideration in the safety assessment of the structural integrity of the vessel. The behavior of such flaws is relevant to the pressurized thermal shock (PTS) scenario and to the plant life extension issue.

There is a dearth of information on the behavior of small flaws in the presence of cladding. This has led at least one RPV integrity study[1] to assume infinitely long flaws (although small flaws are certainly more credible). To date, it is difficult to predict the behavior of finite length flaws for various reasons. An important one is that no criteria exist to predict the evolution of the flaw geometry, thus, only general qualitative estimates can be made in such terms as "there is a tendency for the crack to propagate along the surface." Another important reason is the analytical complexity introduced by the three-dimensional nature of finite length flaws.

It is now an accepted fact in the Oak Ridge National Laboratory (ORNL) Heavy-Section Steel Technology (HSST) Program that, in the absence of cladding, a short flaw will grow to become a long one. Figure 1 shows the variation of the stress intensity factor K_I for an elliptical flaw as a function of the aspect ratio of the major to minor axes (b/a) for the conditions pertaining to the TSE-7 experiment.[2] These curves show that for the initial 19-mm radius semicircular surface flaw used (b/a = 1), the stress intensity factor at the bottom of the flaw is less than that at the surface until b/a exceeds 3. Thus, such a flaw has a tendency to initiate and propagate on the surface to some extent before it can increase in depth. This has indeed been verified experimentally, Fig. 2, which shows the extensive propagation and bifurcation on the surface of the TSE-7 cylinder originating from the semicircular surface flaw. The flaw also increased in depth at many locations to about 30% of the wall thickness.

The question to be investigated is to what extent the existence of tough cladding will restrict propagation of the flaw. If the cladding is sufficiently tough to prevent surface extension of a surface flaw, the flaw is restricted to tunneling, which reduces the potential for further propagation.

A clad-plate research program was conducted as part of the ORNL HSST Program in order to investigate the behavior of small flaws in the presence of cladding.

The objectives of this research were achieved by comparing the load-bearing capacity of clad and unclad flawed plates and by determining the extent of crack propagation in a clad plate as a function of load.

The experimental procedure and results have been presented elsewhere,[3] but, for continuity, a brief description will be repeated below. The results are explained in terms of fracture mechanics concepts.

EXPERIMENT DESCRIPTION

The tests were conducted using a special plate specimen, shown in Fig. 3, whose chemical composition is that of a typical RPV steel conforming to ASTM Specification for Pressure Vessel Plates, Alloy Steels, Quenched and Tempered, Manganese-Molybdenum and Manganese-Molybdenum-Nickel (A 533) Grade B. It was commercially clad using the three-wire series-arc technique and stainless steel type 308, 309, and 312 weld wires. The three-wire series-arc technique was used in some of the older vessels. An autogenous electron-beam (EB) weld is introduced into the base metal to provide a crack initiation site, and at the time a sharp flaw is required, the EB-weld site is hydrogen charged.[4,5] The plate is loaded in four-point bending to approximate the stresses due to PTS.

Two types of tests were performed with these plate specimens. One type of test was performed on plates with preexisting flaws. The purpose of this type of test (termed an "initiation" test), was to determine the critical load at which a flaw initiated. Another type of test was performed on initially unflawed plates. To initiate a flaw, the flaw site was hydrogen charged while the load was maintained constant. This arrangement allowed the load on the plate to be increased beyond the critical load at which a preexisting flaw would have initiated. Such a test with hypercritical loads is termed "arrest" test, and its purpose was to determine the arrest capacity of clad plates with various amounts of stored energy. The flaw, once it initiated from the EB-weld region, (whether from preexisting flaws or flaws initiated under hypercritical loads), either arrested or lead to complete rupture of the plate.

More data were obtained on the load-carrying capacity of flawed plates by reloading plates which did not rupture. Such plates were first heat-tinted at 250 to 350°C to define the arrested flaw shape and were then reloaded until either another pop-in or plate rupture occurred.

TEST RESULTS

Tests on six initially unflawed plates were performed in order to load the plates above the critical load of a flawed plate. This provided varying amounts of energy with which the flaw could challenge the arresting capacity of the cladding (simulated "blunted" flaws). The surface strains (in the uniform bending moment span of the plate) was used as a measure of the amount of energy stored in the system (machine and plate) at the instant the flaw initiated in the EB weld. The target surface strains and corresponding loads for the six plates tested are given in Table 1. All tests on initially unflawed plates were performed at either -25 or 25°C, and Fig. 4 shows the point on the load vs surface-strain curve at which the six plates have been tested. Plate designations shown on the left-hand side of the curve were tested at -25°C, and those on the right-hand side were tested at 25°C. The loads (and strains) were maintained constant under machine ram stroke control during the period of hydrogen charging.

For the first clad plate tested, CP-15, the surface strain was chosen to be approximately the yield strain of the base metal. The flaw propagated but the plate did not rupture. The target surface strain was increased for plates CP-17 and CP-19. In all three cases the flaw initiated and arrested after propagating beneath the cladding a distance that increased with increasing initial load. An unclad plate, CP-21, ruptured when loaded to approximately the base-metal yield strain on the surface. The initial loads, post-arrest loads, and corresponding crack lengths for the four plates tested at room temperature are shown schematically in Fig. 5. It may be noted that as the potential energy stored in the plate increased, the length of the arrested flaw also increased as shown schematically by the shaded flaw shape in Fig. 5. Photographs of actual fracture surfaces of two of the plates are shown in Fig. 6. From these photographs it may be noted that a surface layer composed of heat-affected zone

(HAZ) and cladding arrested the flaw and prevented its propagation along the surface, causing it to tunnel below the surface. Full details can be found in an earlier presentation.[6]

The remaining two clad plates, CP-18 and CP-20, were tested at -25°C in order to obtain data at another point besides room temperature on the arresting capability of the plates. Table 1 also shows the post-arrest loads, however, as discussed later, because of dynamic effects, this is not necessarily the load at the instant the flaw actually arrested.

The loads at various events for two plates with pre-existing flaws, clad plate CP-16 and unclad plate CP-22 are also shown in Table 1. It is interesting to note that the initiation load for plate CP-16 is within 5% of the target load (chosen on the basis of the yield at the surface of base metal) for the "arrest" test for unflawed plate CP-15. The arrested crack shapes also are very similar. Almost the same loads have lead to rupture in both the unclad plates tested. Thus, the critical load for the plates with a flaw corresponding to the shape of the EB weld is approximately 670 kN. The fracture surfaces of these two plates are very similar to those from arrest experiments, and have been presented elsewhere.[7] Thus, the initial load for CP-15 was essentially the critical load, and the critical load for the unclad plate was essentially the same as that for the clad plate.

DISCUSSION

The HAZ was tough enough to prevent surface extension of the flaw for the loads applied. The loads applied, however, were sufficient to result in extensive tunneling beneath the HAZ. Furthermore, the extent of the tunneling was related to the initial load. Moreover, the residual load-bearing capacity of plates, as measured by the critical loads in initiation experiments with fairly large flaws, was generally greater than required to break the unclad plate, even though the test temperatures were lower by 50°C.

The HAZ played a prominent role in enhancing the load-carrying capacity of the clad plates. This may be explained by considering the toughness as measured by the Charpy V-notch (CVN) impact energy. The HAZ is the toughest of the three metallurgical zones of the clad plate specimens at 25°C, while the cladding is toughest at -25°C. CVN impact energy tests were performed on the cladding, HAZ,

and base metal with specimens oriented in a direction corresponding to the EB-induced flaw propagating along the surface of the clad-plate specimens, and the results are shown in Fig. 7. Results of CVN impact testing on specimens oriented in a direction corresponding to the EB-induced flaw propagating in the thickness orientation were similar.[8] The Charpy transition of the HAZ is also noticeably lower than that of the base metal. Results of the ASTM Test for Conducting Drop-Weight Test to Determine Nil-Ductility Transition Temperature (NDT) of Ferritic Steels (E 208) using specimen P-3 resulted in an NDT of 36°C for the base metal.

One of the interesting flaw shapes that occurred in four of the clad plates tested was a result of the flaw extending the entire width of the plate. A typical fracture surface is shown in Fig. 6(b). The flaw had essentially become a long flaw. The stress intensity factor for this case may be estimated by assuming that this geometry is approximately that of a centrally located crack in a finite-width strip loaded by end-moments. The solution for this case is given elsewhere.[9] The load that ruptured the four plates with such a flaw is ~700 kN. The stress intensity factor corresponding to this load is 60 MPa$\sqrt{m}$, assuming that linear elastic fracture mechanics is still applicable.

It is of interest to calculate the average stress ligament on the tensile side of the clad plates. Figure 8 shows the nomenclature used in the following free-body analysis of the forces acting on the plate at the instance of rupture. Figure 8(a) shows schematically typical remaining ligaments in four plates tested (CP-16, -17, -18, -19). The moment of the resultant internal forces acting on the clad plate at the instant of rupture with a flaw extending the entire plate width is given in the small box in Fig. 8(b) as $M = \sigma crd$. The moment of the externally applied machine forces acting on the plate in four-point bending is $M = (Pl)/2$ as shown in Fig. 8(c). Equating the two moments, the average stresses in the unbroken tensile ligament just before rupture is $\sigma = (Pl)/(2crd)$. By using the loads recorded at the moment of rupture during the tests on these plates, the average stress in the unbroken ligament has been estimated, and is given in Table 2. It may be seen that in every case the average stress at rupture is 9 to 30% higher than the average ultimate tensile strength of the composite layer of both cladding and HAZ at the temperature of interest.

Using the K_{Ic}-CVN correlation in the transition-temperature region given by Rolfe and Barsom[10] and the values of the CVN impact energy at -25°C (Fig. 7), K_{Ic} values ranging from 58 to 68 MPa/m were estimated. Thus, a K_I of 60 MPa from the centrally cracked strip is not unreasonable. This may explain why the load on the plate had to be increased to a level that would result in the failure of the remaining ligament when the stresses exceed its ultimate tensile strength.

It is not clear at this time whether cladding alone, without benefit of the tough strong HAZ which played a pronounced role in arresting propagating flaws, would have also elevated the load-bearing capacity beyond that of the unclad plate. In the case of radiation-embrittled reactor pressure vessels, the HAZ will most likely undergo toughness degradation similar to that of the base metal, and would therefore not play such a prominent role in arresting propagating flaws.

It is probable that the post-arrest loads shown in Fig. 5 are controlled by the compliance of the specimen, and are not necessarily the loads at the moment of arrest of the flaw. The crack initiates, propagates and arrests in a time interval that is smaller than that required for the specimen (because of its inertia) to deflect. The crack velocity, measured in one of the plate tests, is approximately 500 m/s. The flaw will therefore propagate the full half-width of the plate, a distance of 0.2 m, in 400 μs. The first natural period of vibration of the plate, approximated as a simply supported beam[11] is 1000 μs. Thus, only after arrest does the new and smaller compliance of the flawed plate allow the plate to deflect further. Because the tests are performed under machine ram stroke control, the load drops to a value controlled by the new compliance of the specimen. The actual load at arrest of the flaw can be higher than the final load shown.

Several factors contributed to the enhanced load-bearing capacity of the clad plates as compared to unclad plates. As previously mentioned, the HAZ was tough enough to prevent surface extension of the flaw for the loads applied, and tunneling occurred. Another factor was the presence of compressive stresses due to bending, which limited the depth to which the flaw could propagate. In the case of an RPV, a severe thermal shock could initiate a flaw and may propagate it beneath the cladding. The integrity of the vessel could then be challenged by the purely tensile stresses created during repressurization.

REFERENCES

1. S. K. Iskander, "A Method of LEFM Analysis of RPV During SBLOCA," *Int. J. Pressure Ves .els Piping* 25, 279-298 (1986).

2. R. D. Cheverton, D. G. Ball, S. E. Bolt, S. K. Iskander, and R. K. Nanstad, *Pressure Vessel Fracture Studies Pertaining to the PWR Thermal-Shock Issue: Experiment TSE-7*, NUREG/CR-4304 (ORNL-6177), Oak Ridge National Laboratory, 1985.

3. S. K. Iskander and R. K. Nanstad, "Observations on the Behavior of Surface Flaws in the Presence of Cladding," pp. 3525-34 in *Advances in Fracture Research*, Proceedings of the 7th International Conference of Fracture (ICF7), Vol. 5, Houston, Texas, March 20-24, 1989, Pergamon Press (1989).

4. D. A. Canonico, J. D. Hudson, "Technique for Generating Sharp Cracks in Low-Alloy High Strength Steels," pp. 60-64 in *Heavy-Section Steel Technology Program Semiann. Prog. Rep. for Period Ending February 28, 1971*, ORNL-4681, Oak Ridge National Laboratory, December 1971.

5. P. P. Holz, *Flaw Preparations for HSST Program Vessel Fracture Mechanics Testing: Mechanical Cyclic Pumping and Electron Beam Weld-Hydrogen-Charge Cracking Schemes*, NUREG/CR-1274 (ORNL/NUREG/TM-369), Oak Ridge National Laboratory, 1980.

6. S. K. Iskander et al., "Crack Arrest Behavior in Clad Plates," pp. 222-242 in *Heavy-Section Steel Technology Program Semiann. Prog. Rep. April-September 1987*, NUREG/CR-4219, Vol. 4, No. 2 (ORNL/TM-9593/V4&N2), Oak Ridge National Laboratory, 1988.

7. S. K. Iskander et al., "Crack Arrest Behavior in Clad Plates," pp. 212-226 in *Heavy-Section Steel Technology Program Semiann. Prog. Rep. October 1987-March 1988*, NUREG/CR-4219, Vol. 5, No. 1 (ORNL/TM-9593/V5&N1), Oak Ridge National Laboratory, 1988.

8. S. K. Iskander et al., "Crack Arrest Behavior in Clad Plates," pp. 169-73 in *Heavy-Section Steel Technology Program Semiann. Prog Rep. October 1986-March 1987*, NUREG/CR-4219, Vol. 4, No. 1 (ORNL/TM-9593/V4&N1), Oak Ridge National Laboratory, 1987.

9. H. Tada, P. C. Paris, and G. R. Irwin, *The Stress Analysis of Cracks Handbook*, 2nd Ed., Paris Productions, Inc., St. Louis, 1985.

10. S. T. Rolfe and J. M. Barsom, *Fracture and Fatigue Control in Structures, Applications of Fracture Mechanics*, Prentice-Hall, New Jersey, 1977.

11. S. Timoshenko, "Vibration Problems in Engineering", D. Van Nostrand, 2 ed. pp. 342 (1937).

Table 1. Test conditions and results for the eight plates tested

Plate	Condition	Type of Test[a]	Load test temperature (°C)	Load (kN)		Surface strain (%)
				Initiation	Post-Arrest[b]	
CP-15	Clad	A	25	676	654	0.31
		I	-25	759	709	
		I	-100	600	R	
CP-17	Clad[c]	A	25	890	823	0.45
		I	-25	756/725	R	
CP-19	Clad	A	25	987	689	0.65
		I	-50	703	R	
CP-21	Unclad	A	25	676	R	0.27
CP-18	Clad	A	-25	823	649	0.39
		I	-25	698	R	
CP-20	Clad	A	-25	868	R	0.41
CP-16	Clad	I	21	703	694	0.3
		I	21	890	738	
		I	-25	698	R	
CP-22	Unclad	I	21	698	R	0.3

[a]A = arrest, I = initiation.

[b]R = plate ruptured in two pieces.

[c]Several pop-ins occurred before rupture.

Table 2. Comparison of tensile stress at rupture of several plates with large flaws to the average ultimate tensile strength of the composite layer of cladding and heat-affected zone

Plate	Test temperature (°C)	Load P (kN)	Average rupture stress (MPa)	Ultimate[a] tensile strength (MPa)
CP-19	-50	703	965	885
CP-17	-25	725	996	760
CP-18	-25	698	959	760
CP-16	-25	698	959	760

[a]Average of the ultimate tensile strength of three-layer cladding and heat-affected zone. Average values of ultimate tensile strengths for cladding and HAZ at -50°C, 870 and 900 MPa, respectively, and at 0°C, 640, and 860 MPa. The values at -25°C were obtained by linear interpolation.

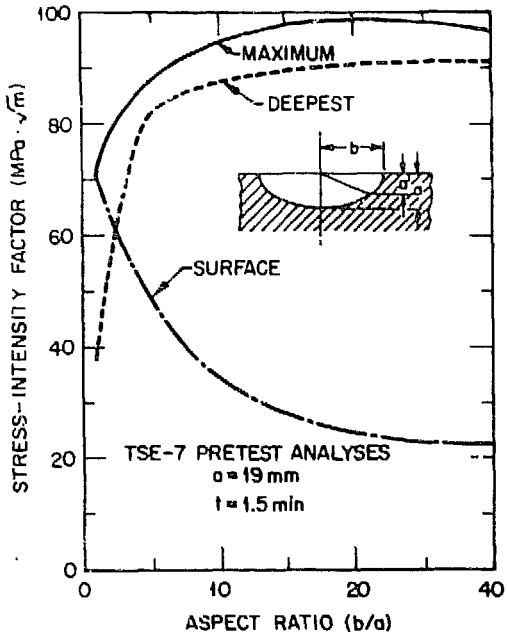

Fig. 1. Variation of the stress intensity factor K_I for an elliptic flaw as a function of the aspect ratio of the major to minor axes (b/a). Source: R. D. Cheverton et al., *Pressure Vessel Fracture Studies Pertaining to the PWR Thermal-Shock Issue: Experiment TSE-7*, NUREG/CR-4304 (ORNL-6177), Oak Ridge National Laboratory, 1985.

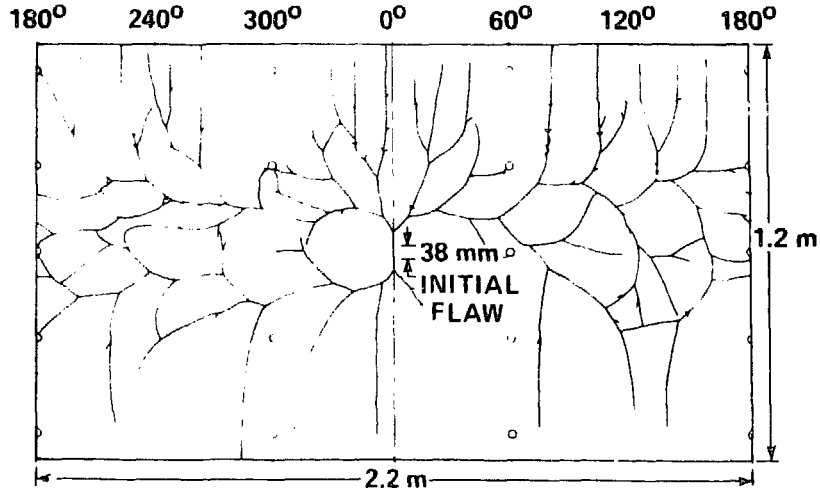

Fig. 2. Developed view of inner surface of the TSE-7 cylinder in which the 19-mm-radius, semicircular flaw propagated on the surface to become a long flaw during the test. Source: R. D. Cheverton et al., *Pressure Vessel Fracture Studies Pertaining to the PWR Thermal-Shock Issue: Experiment TSE-7*, NUREG/CR-4304 (ORNL-6177), Oak Ridge National Laboratory, 1985.

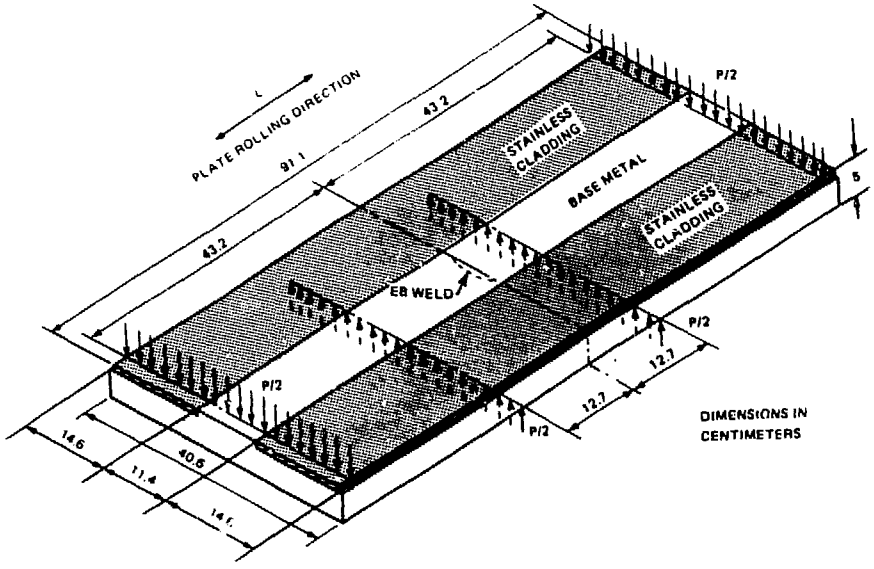

Fig. 3. Clad plate specimen with electron-beam weld tested in four-point bending.

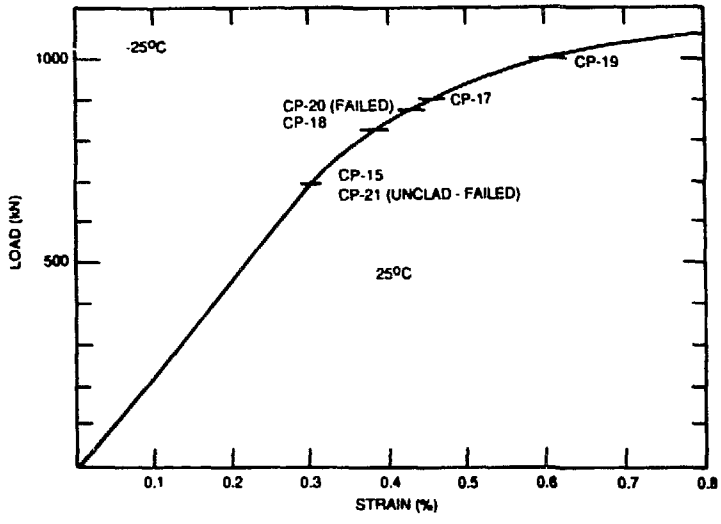

Fig. 4. Point on load vs surface strain curve at which the six plates were tested in the arrest mode. Note that all plates whose designations appear above the curve were tested at -25°C, while those below the curve were tested at 25°C.

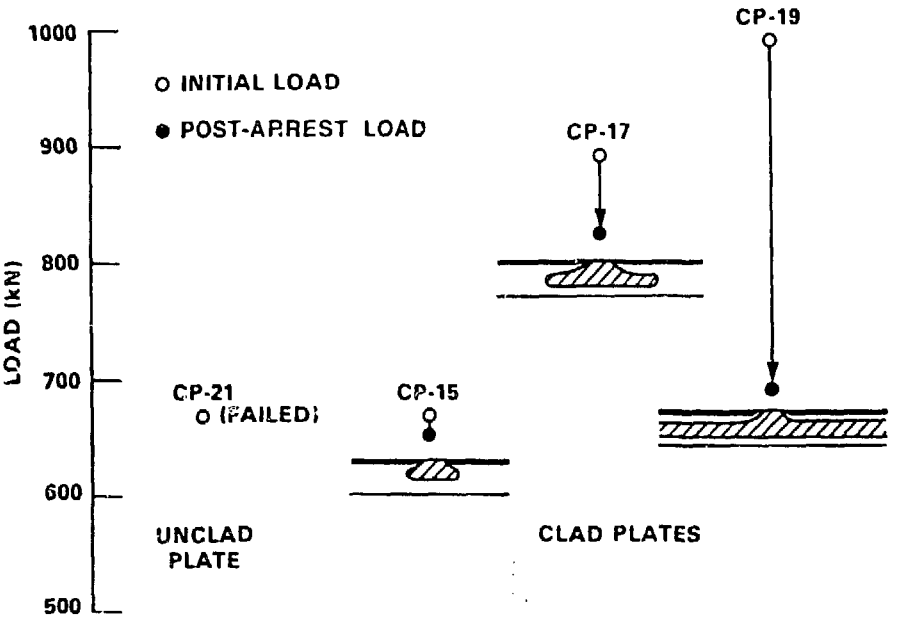

Fig. 5. Initiation loads, post-arrest loads, and corresponding crack lengths for the four plates tested at room temperature.

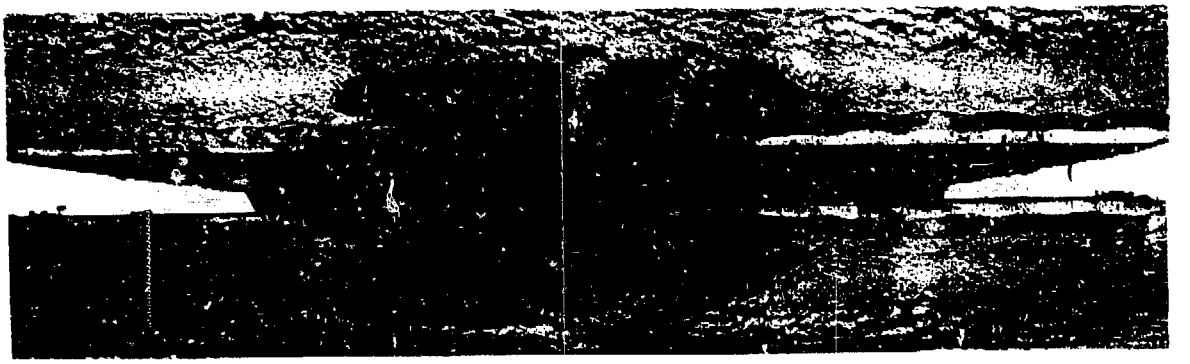

50 mm

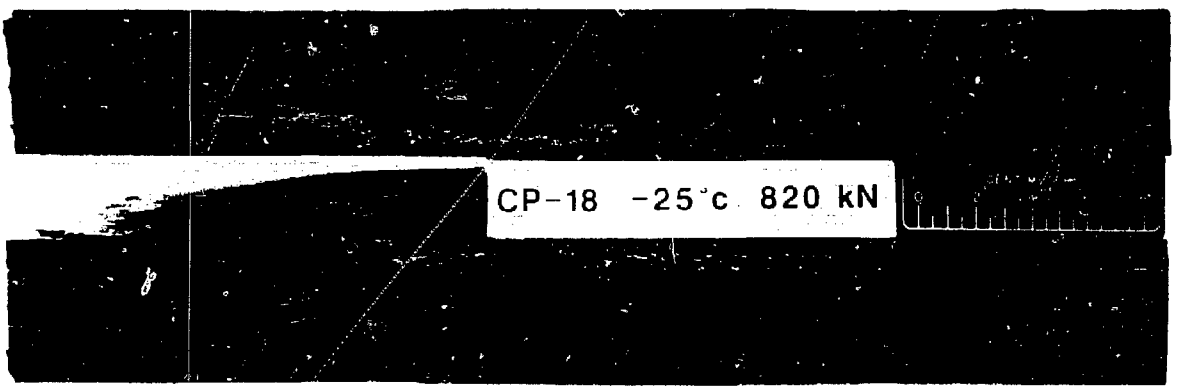

Fig. 6. Fracture surfaces of clad plates (a) CP-17 and (b) CP-18. The dark areas result from hint-tinting after testing and show the arrested flaw shape.

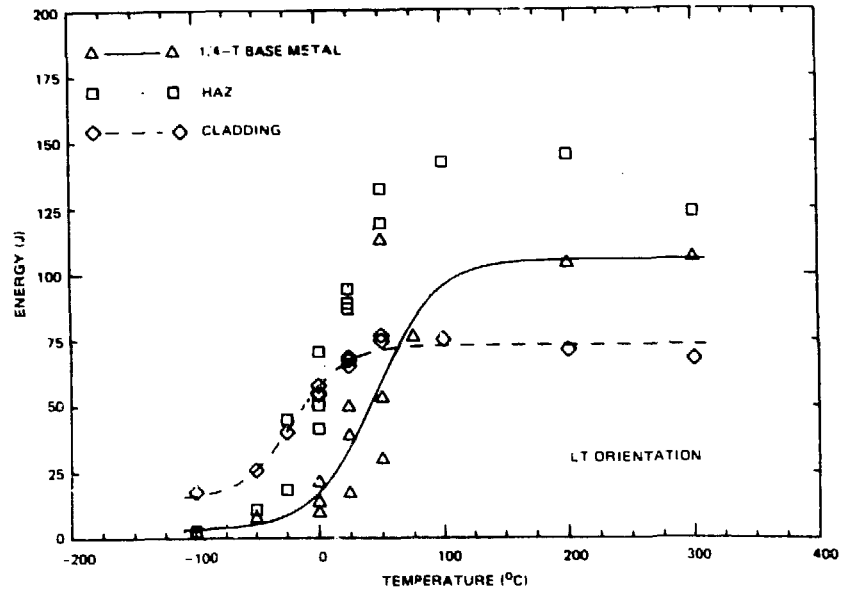

Fig. 7. Charpy impact energy of base metal, HAZ, and cladding used in the clad plates. Specimen orientation corresponds to EB-induced flaw propagating along the surface.

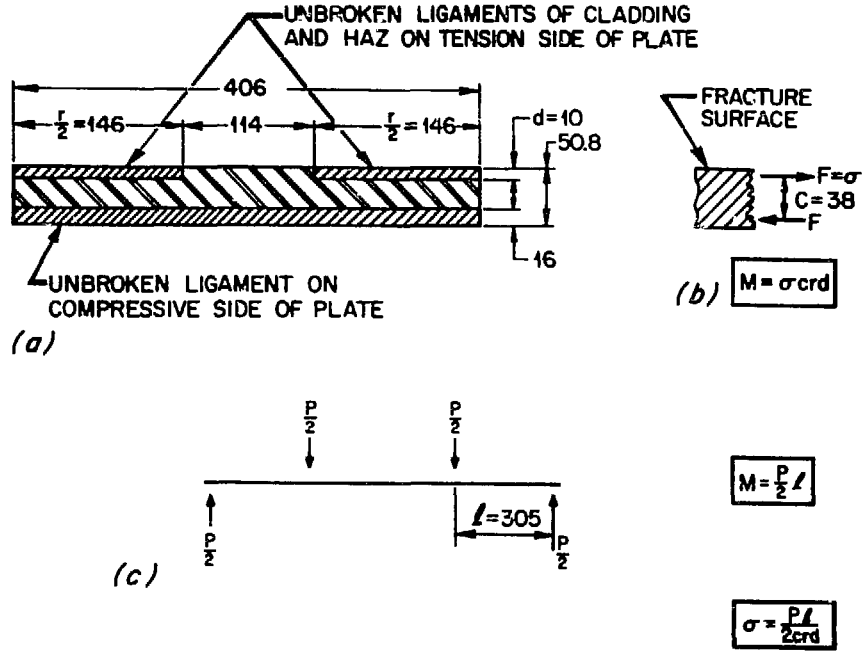

Fig. 8. Analysis of stresses required to rupture the four plates CP-16, CP-17, CP-18, AND CP-19. (a) Idealized, typical remaining ligaments. (b) Forces acting on the fracture surface. (c) Forces and pertinent dimensions of the four-point bend load train.